QUADRUPOLE IONIZATION GAUGE*

by

Helmut Schwarz

Rensselaer Polytechnic Institute
Hartford Graduate Center
East Windsor Hill, Connecticut 06028

Paper to be presented On Invitation
At the Fourth International Vacuum Congress
Manchester, England
April 17 - 20, 1968

*Supported by a NASA grant which is part of NASA Langley Research Center's Vacuum Instrumentation program directed by Paul Yeager.

Quadrupole Ionization Gauge*

HELMUT SCHWARZ

Rensselaer Polytechnic Institute
Hartford Graduate Center
East Windsor Hill, Connecticut 06028 USA

Abstract

The new non-magnetic ionization gauge can be compared with a Penning type ionization gauge where the electrons oscillate along the axis of the tube. The difference between the Penning gauge and the new gauge lies mainly in the fact that the confinement of the electrons is achieved by electrostatic quadrupole lenses instead of a magnetic field. Electrons are emitted from a hot cathode at one end of the tube and accelerated along the tube. They will then encounter an inverted field, since on the other end of the tube a flat disc is positioned which has a potential slightly lower than the cathode potential. This will cause the electrons to return and continue to oscillate obtaining maximum velocity each time they pass the middle of the tube. The produced ions are collected by a cylindrical screen surrounding the whole electrode structure and/or the flat disc. No fast electrons can hit any solids so that the X-ray production is kept very low. The tube can be operated in two modes: 1) d.c. potentials or 2) ultra high frequency (about 200 MHz) are applied to the quadrupole

---

*Supported by a NASA grant which is part of NASA Langley Research Center's Vacuum Instrumentation program directed by Paul Yeager.

rods. In the case of the d.c. operation, the sensitivity factor was by a factor of 10 and in the high frequency operation by a factor of more than 2,000 higher than that of a regular Bayard-Alpert gauge. The X-ray limit is so low that it plays a lesser role than adsorption and desorption phenomena at the ion collector. Adsorption and desorption processes come to an equilibrium in front of the ion collector and create a kind of "gas cloud". This had earlier been postulated as being the main reason of the lower limit of ionization gauges.

1. Introduction

The new non-magnetic ionization gauge consists basically of quadrupole lens systems excited at high frequency. The principle for focusing with a quadrupole system had already been proposed in 1950 in a patent issued to Christofilos (1950). Independently Courant, Livingston and Snyder (1952) have studied the possibility of using alternating-gradient focusing for particle accelerators. Paul and Steinwedel (1953) had proposed this same principle for application in mass-spectrometry. Many papers have come out in the meantime on the subject and a recent survey can be found in a book edited by Septier (1967). The quadrupole radio frequency devices were mostly used for mass filtering. Only recently Dawson and Whetten (1968) have mentioned the possibility of using such a system as an ionization gauge. Already Fischer (1959) had worked out a theory on how to focus electrons with rotationally symmetric quadrupole fields

for possible use as an ionization gauge.

The present work differs substantially from the previous efforts in that the quadrupole tube is operated under such conditions that predominantly electrons are being focused by this kind of strong-focusing device. At the other end of the hot cathode the electrons will encounter a slightly negative potential and therefore, will be driven back. The device is somewhat similar to a Penning type gauge; the electrons are confined in the center of the tube by strong-focusing quadrupole lenses instead of a magnetic field. The ions produced will be collected by a small disc in the center opposite the cathode; this disc provides also the negative potential for the creation of the inverse field.

2. Principle of Operation

Four rods placed symmetrically parallel around the axis of the tube with alternating potential imposed on them will produce approximately the same quadrupole field as the ideal configuration of hyperbolic electrodes sketched on Fig. 1. An a.c. potential $U_o \cos \omega t$ with a superimposed d.c. potential U_{dc} is applied between a pair of opposite "rods". The electric field within the quadrupole is given by:

$$\vec{E} = - \operatorname{grad} \left[\frac{U_{dc} + U_o \cos \omega t}{r_o^2} (y^2 - z^2) \right] \qquad (1)$$

$$m \frac{d^2 y}{dt^2} \vec{j} + m \frac{d^2 z}{dt^2} \vec{k} = - e\vec{E} \qquad (2)$$

which leads to the following differential equations for y and z:

$$\frac{d^2y}{dt^2} - \frac{2e}{mr_o^2}\left(U_{dc} + U_o \cos \omega t\right)y = 0 \tag{3}$$

$$\frac{d^2z}{dt^2} + \frac{2e}{mr_o^2}\left(U_{dc} + U_o \cos \omega t\right)z = 0 \tag{4}$$

Both are of the form of Mathieu's equation (see McLachlan(1947)):

$$\frac{d^2\zeta}{d\theta^2} + \left(a - 2q \cos 2\theta\right)\zeta = 0 \tag{5}$$

the solution of which is given by:

$$\zeta = Ae^{\mu\theta} \sum_{-\infty}^{+\infty} c_\nu e^{i\nu\theta} + Be^{-\mu\theta} \sum_{-\infty}^{+\infty} c_\nu e^{-i\nu\theta} \tag{6}$$

which can be applied for ζ being either y or z. In the first case (eq. 3)

$$a = a_y = -\frac{8eU_{dc}}{r_o^2\, m\omega^2} \tag{7}$$

and in the second (eq. 4)

$$a = a_z = +\frac{8eU_{dc}}{r_o^2\, m\omega^2} \tag{8}$$

and in both cases

$$q = \frac{4eU_{dc}}{r_o^2\, m\omega^2} \tag{9}$$

which results from the fact that the time operator $\frac{d^2}{dt^2}$ has to be replaced by the operator $\frac{4}{\omega^2}\frac{d^2}{d\theta^2}$, since $\theta = \frac{\omega t}{2}$. The characteristic exponents

μ of the solution can be determined from a and q. But in order that y and z be real, μ has to be purely imaginary of the form $\mu = \frac{b}{d} i$, where b and d are integral numbers. The upper limits for a_z and the lower limits for a_y respectively for which these conditions exist are represented by the two curves on Fig. 2. a_z and a_y are already given in units of U_{dc} as a function of the peak voltage U_o for electrons and at a high frequency of ν = 200 MHz as applied to the rods. So that only electrons remain on a stable trajectory one has to stay close to the two points of the two curves which yield $a_y = -a_z$. This is the case approximately at U_Φ = 160 volts, which then fixes the value for U_{dc} = 27 volts. For values of U_o >160 volts one can also have stable trajectories for electrons but other charged particles with higher masses M may also become stable. The dc potential U_{dc} to be then applied can be determined from the intersection of the line as given by: $U_{dc} = -\gamma U_{o1}$ with the lower curve of Fig. 2. γ is smaller than 0.166 and U_{o1} varies between O and U_o. From the corresponding value for U_{o1} one can find out the range of masses up to which stable conditions exist. All charged particles with atomic weights smaller than

$$A = 5.45 \times 10^{-4} \, U_o/U_{o1} \qquad (10)$$

then fulfill these conditions for the constructed device with r_o = 1 cm and ν = 200 MHz. For ions with A = 1 (hydrogen) a ratio of $\gamma U_o / U_{dc} \approx 1840$ would be necessary which shows that with $\gamma < 0.166$ practically only electrons

will oscillate under stable conditions. Due to the long electron path the amount of ions produced will be much higher than in a normal ionization gauge.

3. Gauge Design and Electrical Circuit

The schematics of the quadrupole ionization gauge with its electrical connections are depicted on Fig. 3. The four rods R provide the alternating high frequency field. Electrons are emitted from the hot cathode C which consists of a pure tungsten wire in hairpin shape. At the anode ring (AR) the potential U_{dc} is applied and serves mainly to detect the electron emission i^- in an amperemeter A before the high frequency is set in operation. The collector disc Co has a potential V_s negative against the cathode. Ions being collected at Co are measured as a current i^+ with an electrometer type nanoammeter (nA).

In order to avoid transmission losses at the relatively high frequency, the two pairs of the quadrupole rods were used as transmission lines for the high frequency. This is not shown on Fig. 3. In order to get the peak to peak voltage between the two pairs of rods, an appropriate impedance (not shown on Fig. 3) had been inserted at the other end of the rods. The whole electrode structure is enclosed by a cylindrically shaped screen which is on ground potential as is the positive side of the cathode C heated by a low voltage DC power supply U_h. The peak voltage U_o is also measured by an RF-voltmeter not shown on Fig. 3.

4. Calibration of Gauge

It was possible to find the conditions under which the ion current i^+ was proportional to the pressure p and the electron current i^- as this latter was determined before the RF generator had been set in operation.

The pressure p was determined with a Redhead gauge. The vacuum was produced with an Ultek-ion pumping system which had been rough-pumped with a cryopump. Stainless steel had been used throughout for the construction of the vacuum system. Copper gaskets for the flanges and valves had been used that could be baked out up to 450° C. After proper ultra high vacuum treatment an ultimate vacuum of 10^{-13} Torr could be obtained. Calibration was performed with dry air and argon.

Figure 4 shows a family of curves giving a relationship as measured between the ion current i^+ and the collector potential V_s for different pressures of dry air as parameters starting from 2×10^{-5} Torr down to 5×10^{-8} Torr. For the optimum collector potential of about $V_s = -19.5$ volts the gauge constant C as defined by:

$$Cp = i^+/i^- \qquad (11)$$

revealed a value of $C \approx 10^4$ Torr^{-1}. Under d.c. conditions, which means the rods were only on the potential U_{dc}, this constant did not exceed a value of $C \approx 50$ Torr^{-1}. This is a factor of 10 higher than the VEECO-type Bayard-Alpert gauge.

5. Lower Limit

The lower limit for the RF operation could not yet be determined. Down to 10^{-13} Torr still a linearity between pressure p and ion current i^+ could be observed. However, quite a pumping action could be found and there are indications that the lower limit is not determined by X-rays eventually produced by the slow electrons, but rather by absorption and desorption processes at the collector electrode. These processes enter into an equilibrium in front of the ion collector and create a kind of "gas cloud" as this had earlier been postulated by Schwarz (1951) and apparently later observed by Redhead (1966). Such a gas cloud being in a steady state may be the main effect that determines the lower limit long before the X-ray limit shows up.

6. Acknowledgment

The skillful technical assistance of H. A. Tourtellotte is gratefully acknowledged. The author is also thankful to the Organizing Committee for their kind invitation to present this paper at the "Fourth International Vacuum Congress" in Manchester, England.

7. References

CHRISTOFILOS, N. C. (1950). U.S. Patent, 2,736,799 (issued Feb. 28, 1956)

COURANT, E. D., LIVINGSTON, M.S., and SNYDER, H.S., 1952, Phys. Rev. 88, 1190-1196.

DAWSON, P. H. and WHETTEN, N.R., 1968, J. Vac. Sci. Technol. 5, 1-18.

FISCHER, E., 1959, Z. Physik 156, 1-26.

McLACHLAN, N. W., (1947). "Theory and Application of Mathieu Functions" Oxford University Press (Clarendon), London, and New York.

PAUL, W. and STEINWEDEL, H. 1953, Z. Naturforsch. 8a, 448-450.

REDHEAD, P. A., 1966, Trans. 13th Vac. Symposium, pp. 67-68.

SCHWARZ, H., 1951, Arch. Techn. Messen (ATM) V-1341-2 (see also HAEFER, R. 1955, Acta Physica Austriaca 9, p. 200 referring to this paper).

8. Figure Captions

Fig. 1 - Ideal Electrode Configuration for Quadrupole Field

Fig. 2 - Stability Limits for Quadrupole Field
Units in volts for electrons, r_o = 1 cm and
ν = 200 MHz

Fig. 3 - Schematics of Quadrupole Ionization Gauge and Electrical Circuit

Fig. 4 - Ion Current i^+ as a Function of Collector Potential V_s at differeht pressures p of dry air for U_o = 160 volts, U_{dc} = 27 volts, ν = 200 MHz

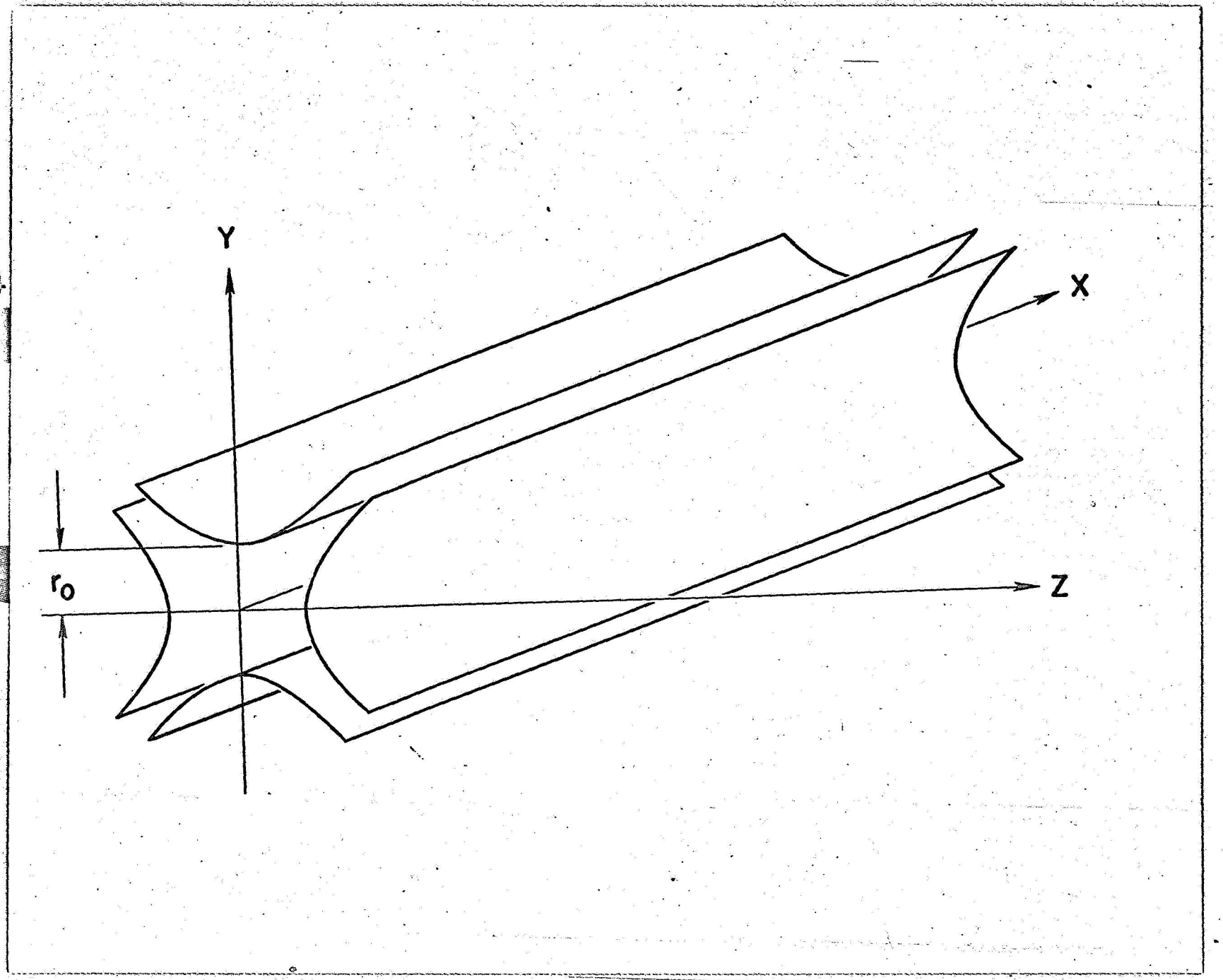

Fig. 1

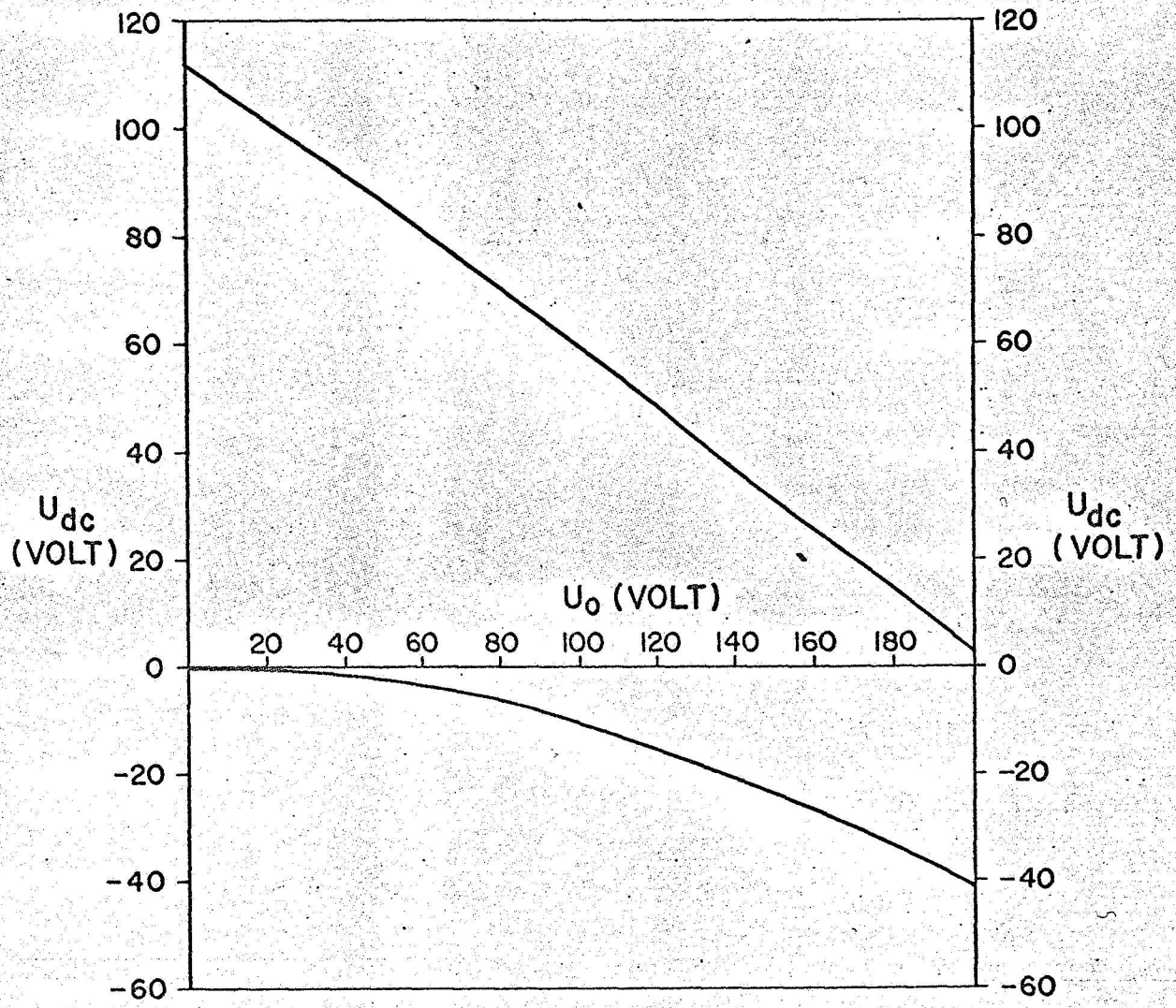
120
100
80
60
40
20
0
-20
-40
-60
U_{dc} (VOLT)
U_0 (VOLT)
20 40 60 80 100 120 140 160 180

Fig. 2

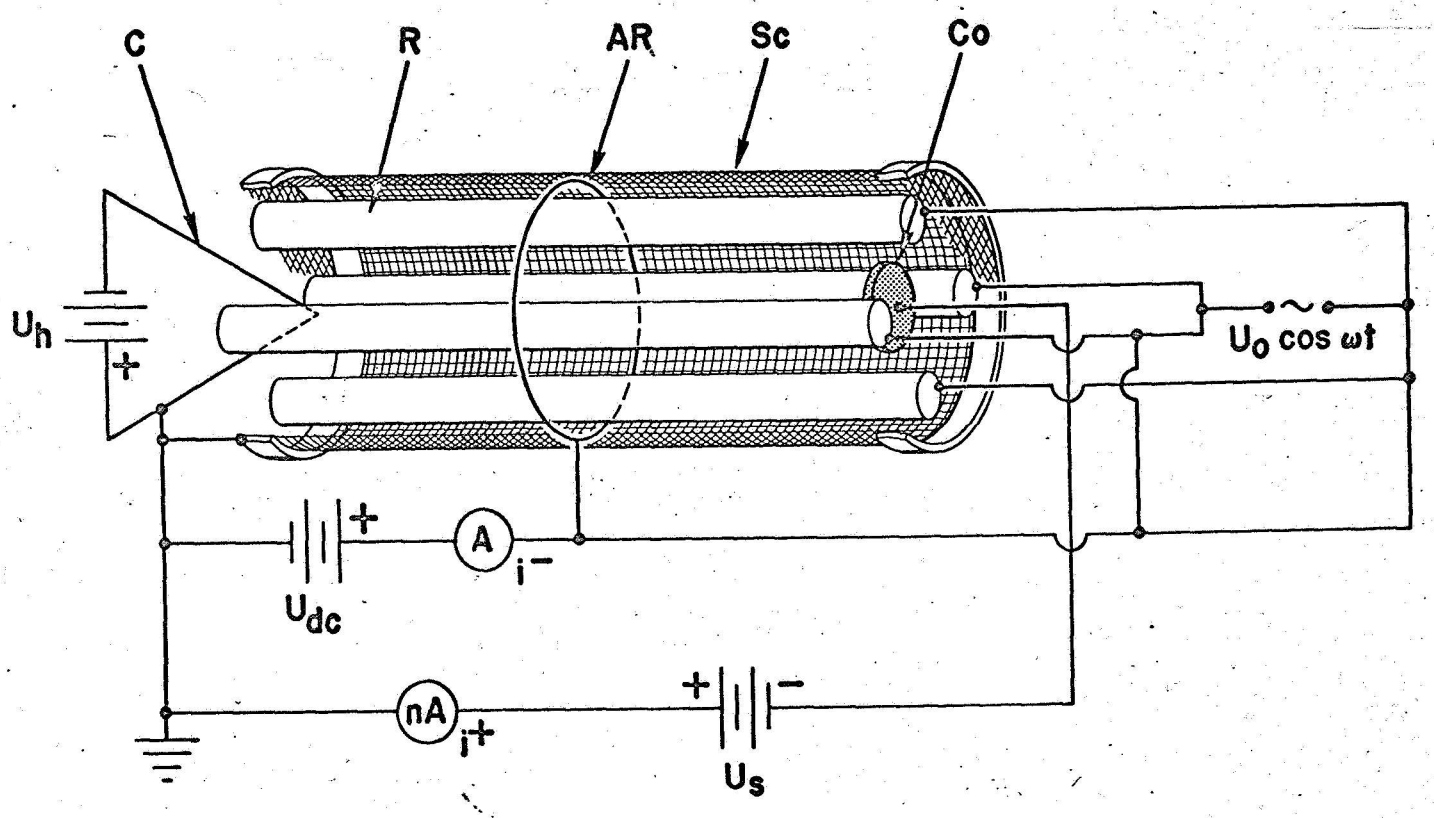

Fig. 3

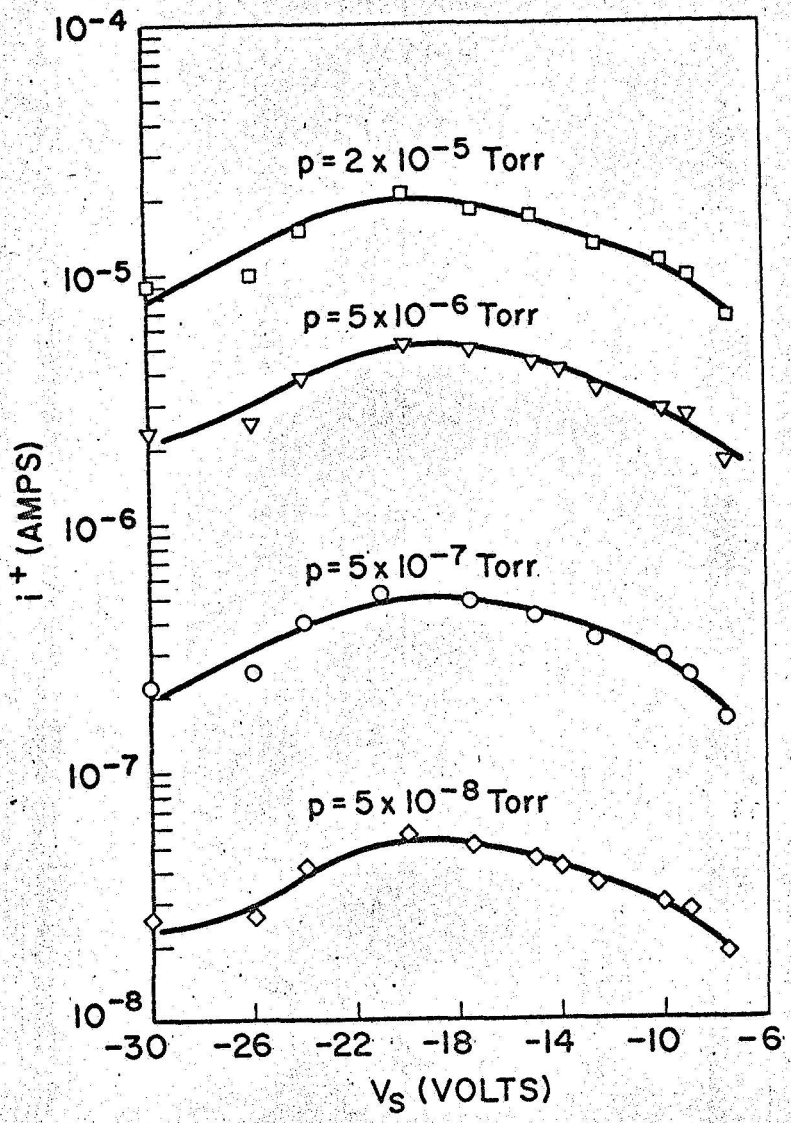
10^{-4}
10^{-5}
10^{-6}
10^{-7}
10^{-8}
i^+ (AMPS)
$p = 2 \times 10^{-5}$ Torr
$p = 5 \times 10^{-6}$ Torr
$p = 5 \times 10^{-7}$ Torr
$p = 5 \times 10^{-8}$ Torr
-30
-26
-22
-18
-14
-10
-6
V_S (VOLTS)

Fig. 4